

HICO Calibration and Atmospheric Correction

Curtiss O. Davis

**College of Earth Ocean and Atmospheric Sciences
Oregon State University, Corvallis, OR, USA 97331**

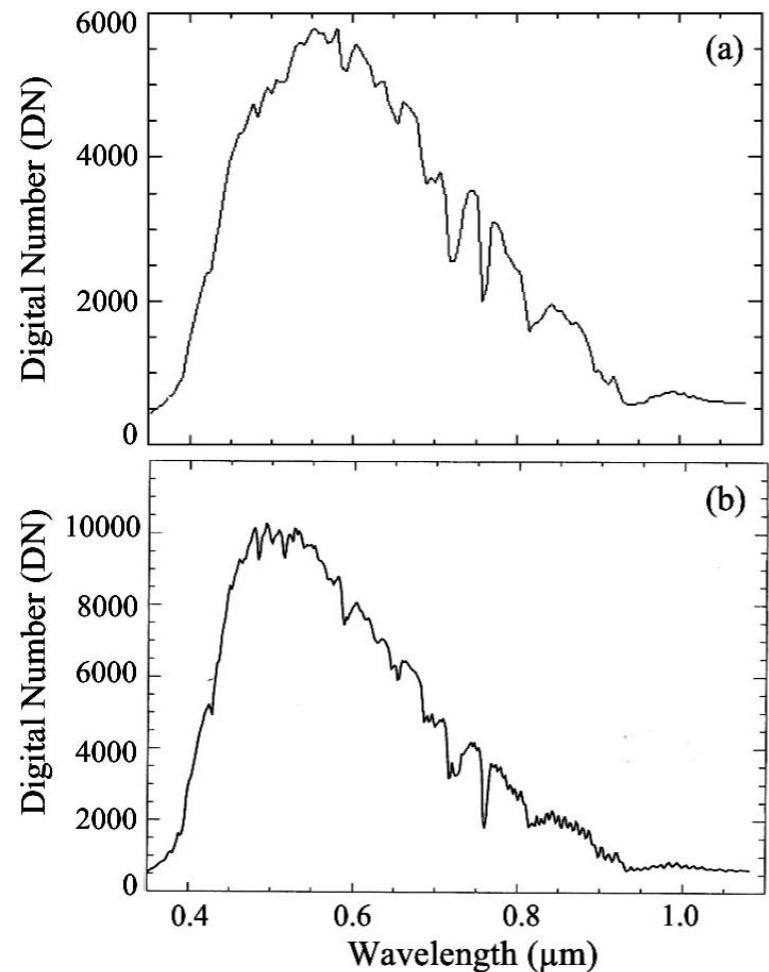
cdavis@coas.oregonstate.edu



- HICO calibrated radiances
 - On orbit Maintenance of calibration
- Atmospheric correction
 - Cloud shadow
 - NASA
 - ATREM and Tafkaa
- Discussion

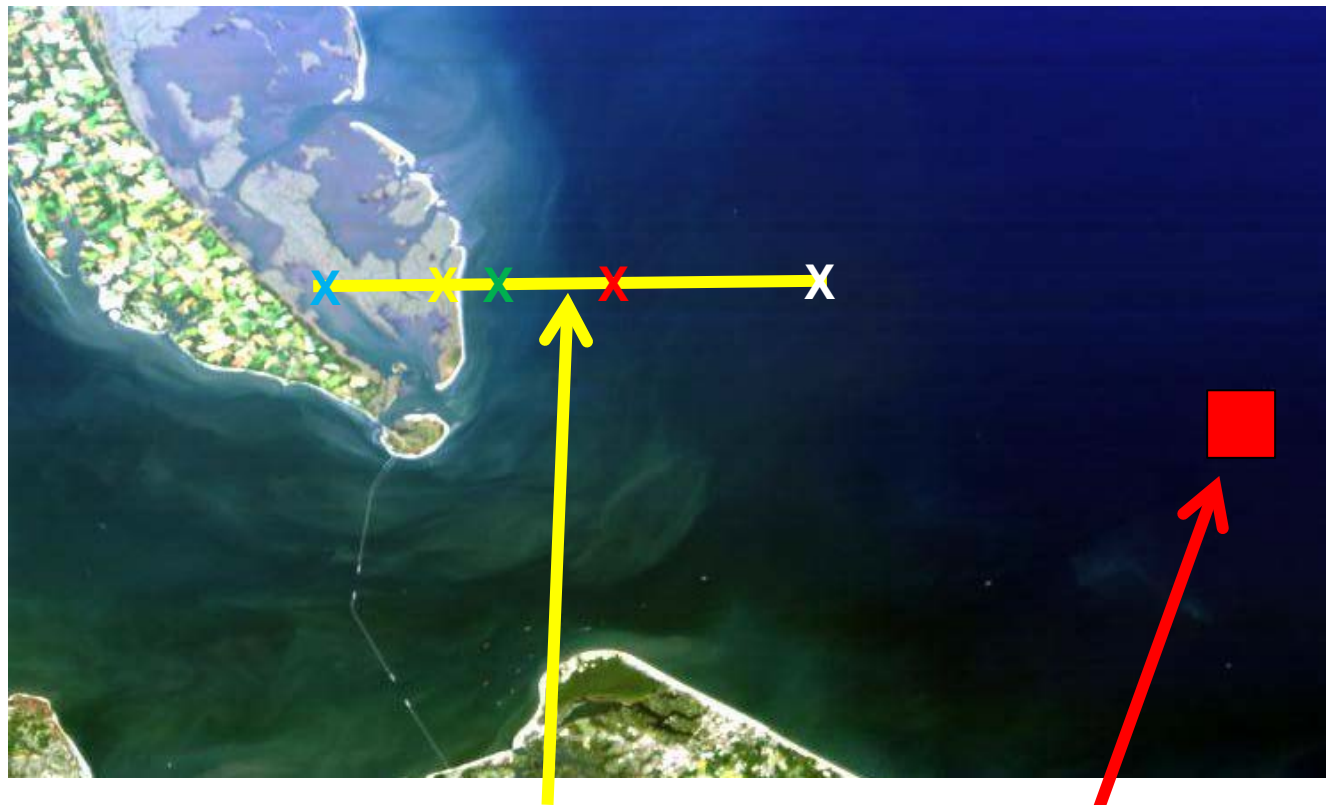
HICO On-Orbit Calibration

- HICO fully calibrated in the laboratory (Lucke et al, 2011)
 - Radiometric calibration
 - Spectral calibration
 - Dark current correction
 - Second Order correction
- HICO does not have a second order filter or an on-board calibrator.
- Cannot ask the ISS to rotate to point at the moon.
- On-orbit calibrations using natural scenes (Gao et al, 2012)
 - Spectral calibration using Fraunhofer lines and oxygen line
 - Radiometric calibration using land calibration targets
 - Second order correction using water scenes



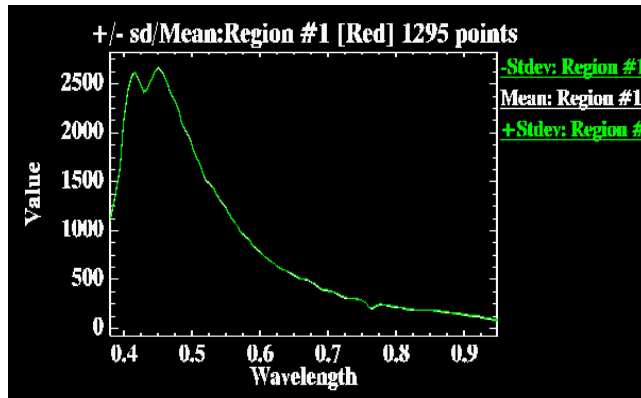
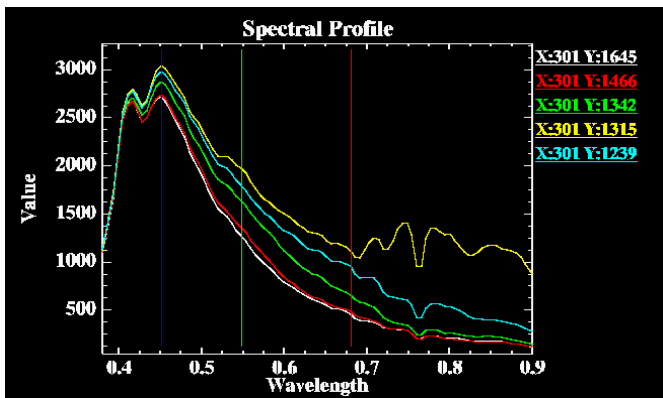
HICO spectra a) normal (5.7 nm) resolution and b) at full (1.9 nm) resolution used for spectral calibrations.

Calibrated Spectral Radiances



Left: Spectra extracted from pixels along the east-west transect shown in yellow. Approximate locations of the spectra are indicated by same color Xs on the image. Spectra are scaled calibrated at-sensor radiances.

Right: Mean and standard deviation of 1295 pixels in the red Region of Interest. The SNR (μ/σ including all sensor and environmental variations) is $>300:1$ for much of the spectra. Spectra are scaled calibrated at-sensor radiances.



Radiometric Comparison of HICO to MODIS (Aqua)

Nearly coincident HICO and MODIS images of turbid ocean off Shanghai, China demonstrates that HICO is well-calibrated

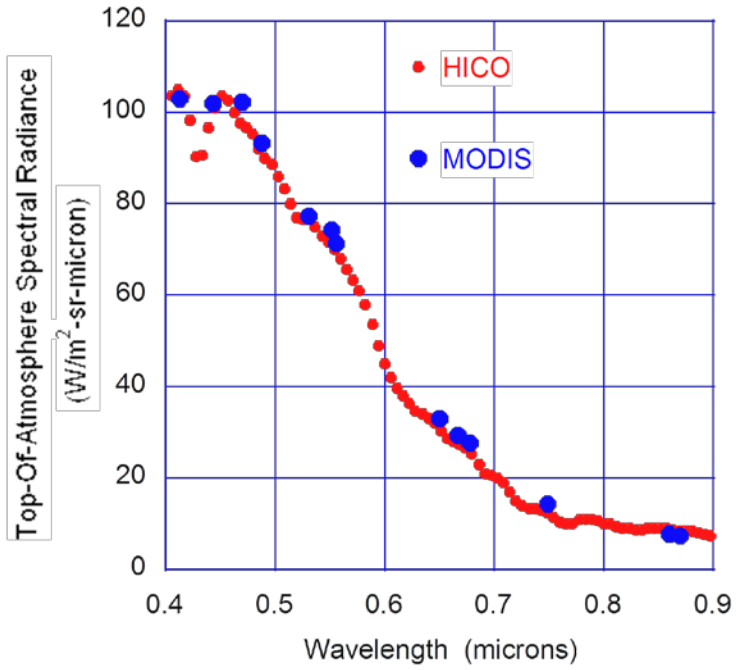
HICO
 Date: 18 January 2010
 Time: 04:40:35 UTC
 Solar zenith angle: 53°
 Pixel size: 95 m

MODIS (Aqua)
 Date: 18 January 2010
 Time: 05:00:00 UTC
 Solar zenith angle: 52°
 Pixel size: 1000 m

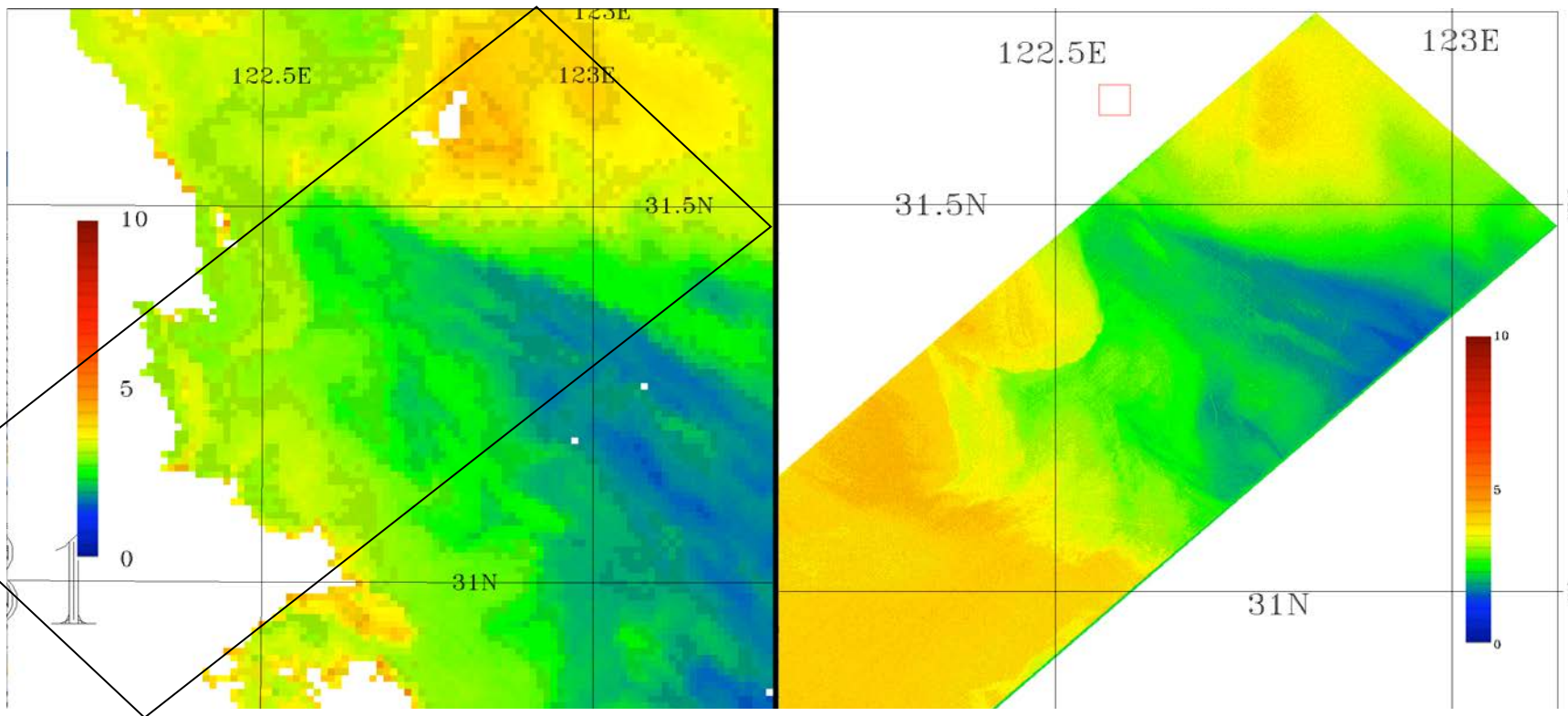
East China Sea off Shanghai



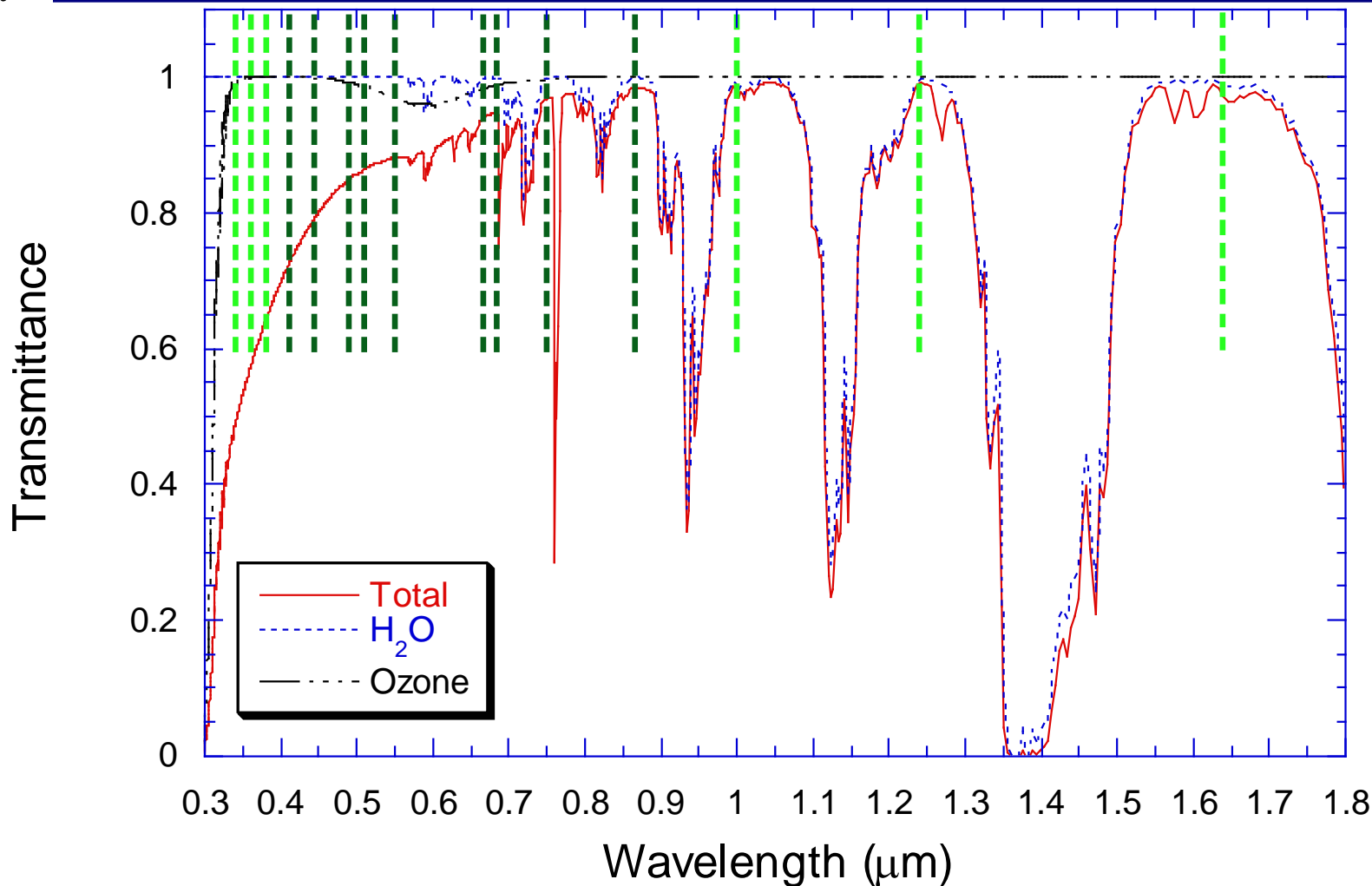
Top-Of-Atmosphere Spectral Radiance



Chlorophyll Comparison of HICO to MODIS (Aqua)



Nearly coincident MODIS and HICO™ images of the Yangtze River, China taken on January 18, 2010. Left, MODIS image (0500 GMT) of Chlorophyll-a Concentration (mg/m³) standard product from GSFC. The box indicates the location of the HICO image relative to the MODIS image. Right, HICO™ image (0440 GMT) of Chlorophyll-a Concentration (mg/m³) from HICO™ data using ATREM atmospheric correction and a standard chlorophyll algorithm. (R-R Li and B-C Gao.)

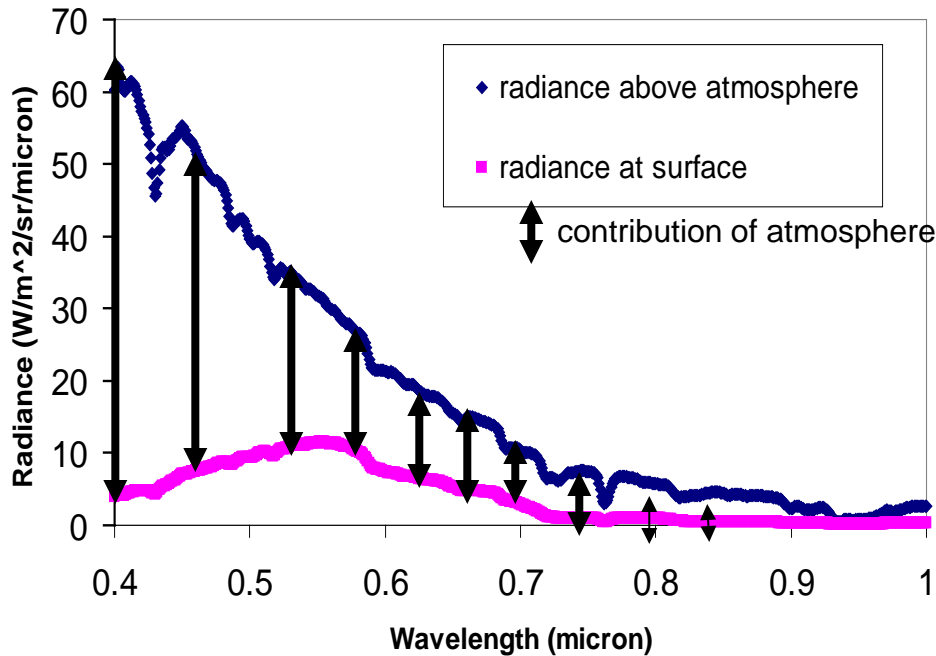


- Multispectral channels selected to avoid water vapor and other absorptions
- Must correct the full spectrum for hyperspectral data

Figure From Menghua Wang, NOAA/NESDIS/STAR

Difficulty of Atmospheric Removal over water

Radiance calculated from measured coastal spectrum



- Atmosphere most of signal
- Atmospheric gasses are well mixed, well understood
- Water is variable
- Aerosols variable in space & time
- Accurate aerosol models and radiative transfer necessary

- Tafkaa-6-S
 - Based on ATREM (Gao & Davis 1997 PROC SPIE)
 - Uses 6-S atmospheric model
 - User selects aerosol model and optical depth
 - Handles data from all altitudes
 - Changes from ATREM include ability to parse image header file, improve speed, use larger set of aerosol models
- Tafkaa-Tabular
 - Much of the code based on ATREM (Gao & Davis 1997, PROC SPIE)
 - Changes as listed above plus:
 - Uses a large look-up table for the aerosol correction
 - Table created using Zia Ahmed's full vector radiative transfer model
 - Can use dark pixel assumption for open ocean scenes
 - Includes a correction for reflections off of the sea surface
 - Only works for near sea-level data
 - Originally described in (Gao, Montes, Ahmad, & Davis, Applied Optics 2000), modifications in several SPIE proceedings

Tafkaa Atmospheric Correction

The apparent reflectance ρ_{obs}^* at a hyperspectral sensor for a given wavelength is

$$\rho_{\text{obs}}^* = \pi L_{\text{obs}} / (\mu_o F_o) \quad (1)$$

where L_{obs} is the radiance of the ocean–atmosphere system measured by the sensor, μ_o is the cosine of the solar zenith angle, and F_o is the extraterrestrial downward solar irradiance at the top of the atmosphere. Then ρ_{obs}^* can be expressed as:

$$\rho_{\text{obs}}^* = T_g [\rho_{\text{atm+sfc}}^* + \rho_w t_d t_u / (1 - s \rho_w)] \quad (2)$$

where T_g is the total atmospheric gaseous transmittance on the sun–surface–sensor path, $\rho_{\text{atm+sfc}}^*$ is the reflectance resulting from scattering by the atmosphere and specular reflection by ocean surface facets, t_d is the downward transmittance (direct + diffuse), t_u is the upward transmittance, s is the spherical albedo that takes into account the reflectance of the atmosphere for isotropic radiance incident at its base, and ρ_w is the water- leaving reflectance. Solving (2) for ρ_w yields

$$\rho_w = \rho_{\text{obs}}^* / T_g - \rho_{\text{atm+sfc}}^* / [t_d t_u + s (\rho_{\text{obs}}^* / T_g - \rho_{\text{atm+sfc}}^*)] \quad (3)$$

Given L_{obs} , the water-leaving reflectance can be derived according to (1) and (3) and the other quantities in the right hand side of (3) modeled theoretically.

Tafkaa-Tabular Look-up Table Generation

We use a modified version of the Ahmad and Fraser code to generate lookup tables for retrieving the required atmospheric parameters. This code includes an atmospheric layering structure that allows for the proper mixing of aerosol particles with atmospheric molecules and the treatment of wind-roughened water surfaces.

The lookup table quantities $\rho^*_{\text{atm+sfc}}$, t_d , t_u , and s are functions of wavelength (λ), solar zenith angle (θ_o), view zenith angle (θ), relative azimuth angle ($\varphi - \varphi_o$), aerosol model, optical depth (τ_a), and surface wind speed (W). The values of $\rho^*_{\text{atm+sfc}}$ in our lookup table are obtained for a total of 25 aerosol models, 16 MODIS channels, and for the following values of independent variables:

τ_a 0, 0.1, 0.2, 0.3, 0.5, 0.7, 1.0, 1.3, 1.6, and 2.0 at 0.55 μm ;

θ_o 1.5°, 12°, 24°, 36°, 48°, 54°, 60°, 66°, and 72°; 193

θ 0°, 1.5°, 6°, 12°, 18°, 24°, 30°, 36°, 42°, 48°, 54°, 60°, 66°, 72°, 78°, 84°, and 88.5°;

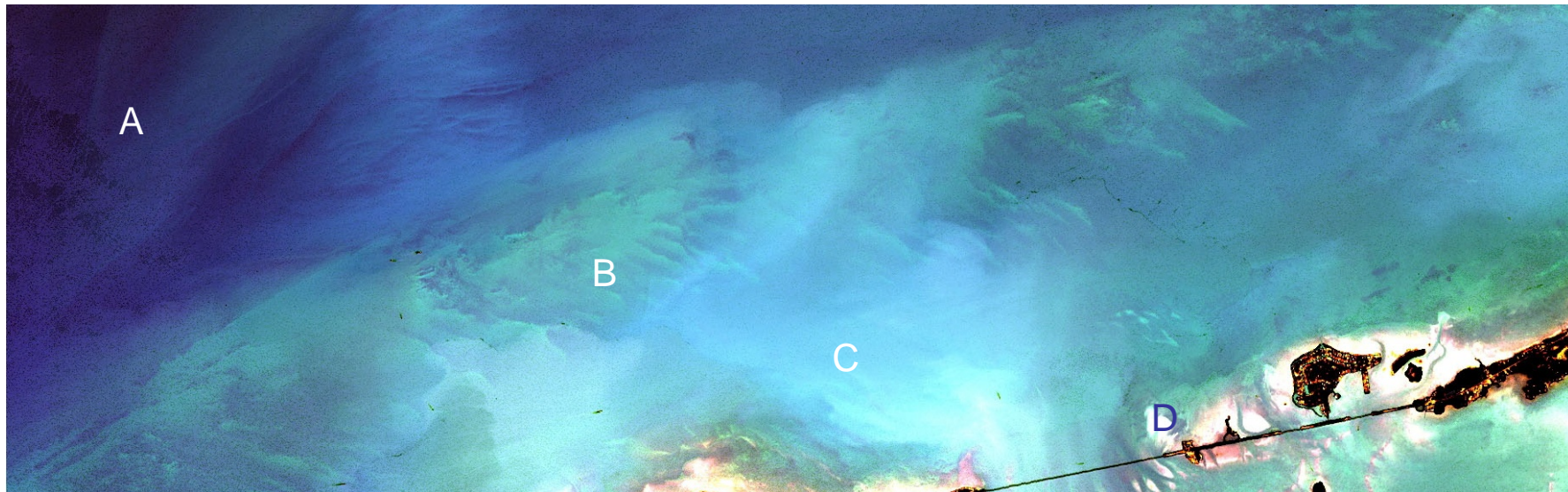
φ_o 0;

φ 0°, 12°, 24°, 36°, 48°, 60°, 72°, 84°, 90°, 96°, 108°, 120°,

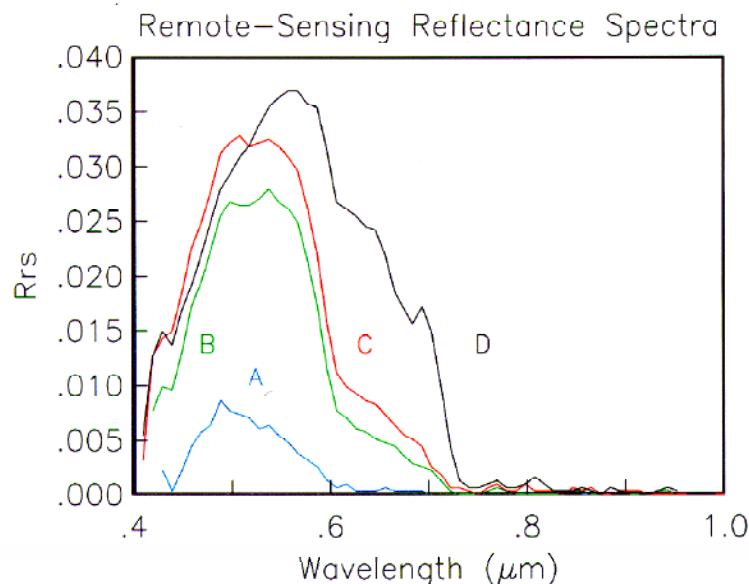
132°, 144°, 156°, 168°, and 180°;

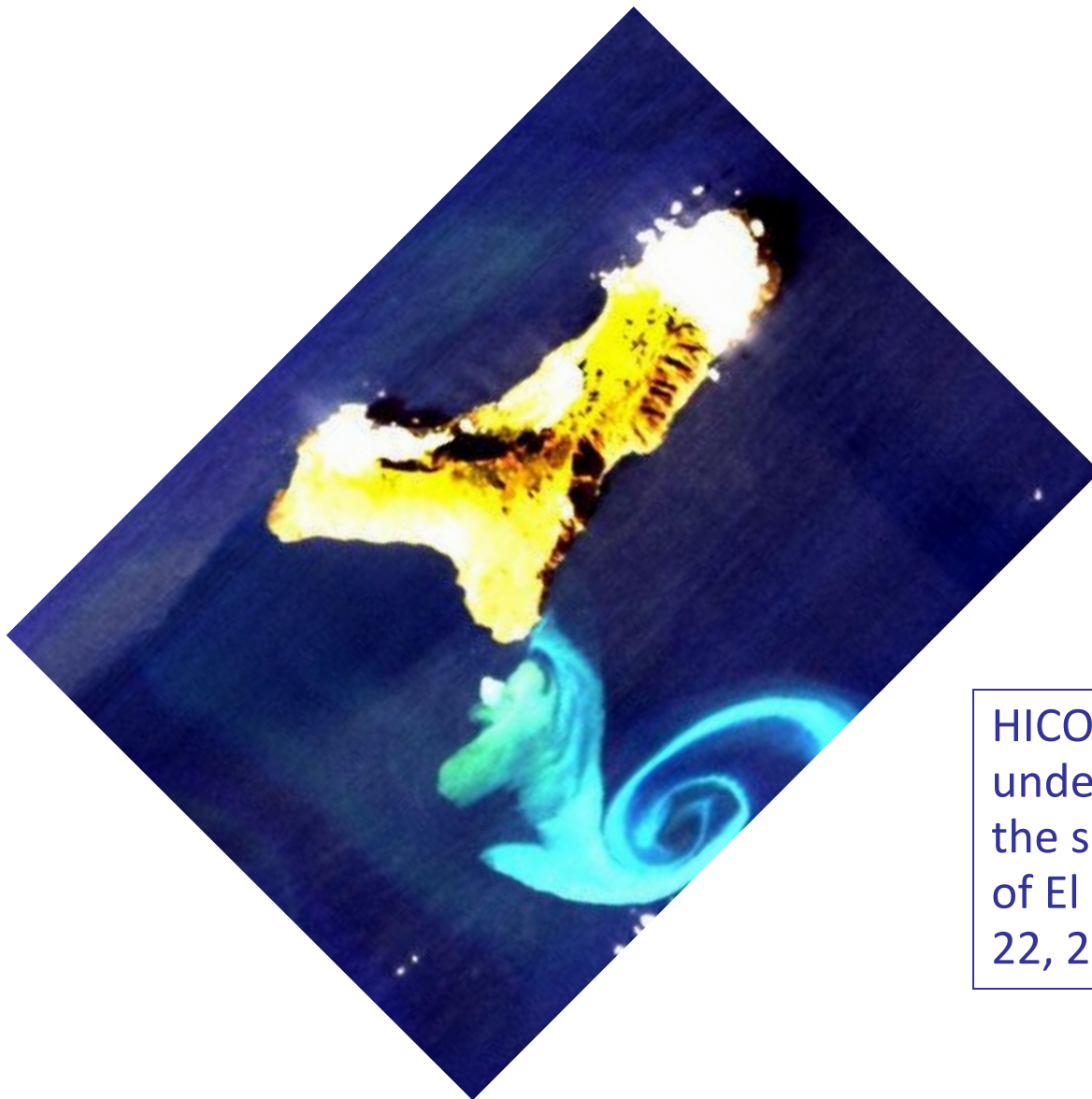
W 2, 6, and 10 m/s;

Tafkaa Tabular Including Surface Glint Correction for Ocean Scenes



AVIRIS data were atmospherically corrected using the Tafkaa Tabular algorithm for ocean scenes. The data are corrected for skylight reflected off the sea surface and then it is assumed that the water leaving radiance is 0 for wavelengths greater than 1.0 micron. (Gao, et al., *Appl. Opt.* 39, 887-896, 2000)





HICO Image of the new underwater volcano off the small Canary Island of El Hierro, December 22, 2011.